NIKHEF

NATIONAAL INSTITUUT VOOR KERNFYSICA EN HOGE-ENERGIEFYSICA

NIKHEF-H/94-12

# A test of four microstrip gas counters in a high rate muon beam

M.H.J. Geijsberts, F.G. Hartjes, J.C.D.F. Rövekamp, F. Udo and A.R. de Winter
NIKHEF, Amsterdam, The Netherlands

M. Bruijn and A.C.M. Snijders
SRON, Utrecht, The Netherlands

G. Gracia
GAES, University of Santiago, Spain



April 1994

***Abstract***

*Four Micro Strip Gas Counters (MSGC) with a sensitive surface of 10x10 $cm^2$ have been tested in a 100 GeV/c muon beam of up to $2x10^7$ particles/s at the CERN SPS. Each counter contained 500 anode and 500 cathode strips of 10 cm long. The signals were processed by VLSI preamplifiers directly mounted onto the detector board. Read out of the analogue signals was done serially into an FADC. Results are given for the efficiency, homogeneity, resolution and the count rate capability of these detectors.*

## 1. Introduction

The MicroStrip Gas Counter(MSGC) is a recently developed variety on the multiwire proportional counter [1]. The wires are replaced by strips etched in a metal layer that is deposited onto an insulating substrate. The etching pattern contains cathode strips interspersed between anode strips to create an electrical field near the anodes that is high enough to cause electron multiplication. The gas volume above the strip plane is limited by a negatively charged electrode to drift the electrons, which are freed in the gas above the substrate, down towards the multiplication region. Fig. 1 shows the layout of the substrate and the gas region above it. The best performance of the counter is reached for particles traversing perpendicularly through the plane of the substrate. In this case the dimension of the electron cloud at arrival on the substrate is only given by diffusion. Several groups [2, 3, 4] have shown that this detector is capable of detecting minimum ionising particles with good accuracy and efficiency. A program is started at CERN [5] to develop these detectors regarding radiation hardness and reliability and to establish production facilities, especially in view of application at the future large hadron collider.

The test described below was done to examine the feasibility of using the present MSGCs with 512 preamplifier channels and a sensitive area of 10 x 10 $cm^2$ as a vertex detector for the Spin Muon Collaboration experiment (NA 47) at CERN. This vertex detector will contain in total 16 MSGC planes.

A special point of investigation was whether the preamplifiers (RAL type MX5) would survive the small scale gas discharges that inevitably occur in this kind of detectors, since they were only developed for the silicon microstrip detector in DELPHI [6]. For the test a batch of four MSGCs was examined:

a. in the halo of the beam ($10^3$ muons/s)

b. in the full beam ($2x10^7$ muons/s).

## 2. Set-up

The sensitive area of the counters consisted of 496 cells with a 200 μm pitch. Each cell contained an anode strip of 7 μm wide and a cathode strip of 90 μm wide. The length of the strips was 96 mm, while the gap between anode and cathode was 52 μm. The pattern was etched into an Aluminium layer of 1 μm thickness, which was deposited onto a 300 μm thick borosilicate substrate[7]. The backside of the glass was left blank. The substrate was glued onto a support board, which carried the preamplifier chips, the digital receivers of the control signals and the drivers of the analogue output signal. Fig. 2 shows a photograph of the assembly of the detector with the electronics.

The gap between drift cathode and substrate was 2.7 mm wide and filled with DME/$CO_2$ 60/40. This mixture is known to give a good efficiency and enables a high drift speed under a high electrical field [4]. A drawback of this mixture that showed up in the test, was that the diffusion of the drifting electrons was insufficient to produce an electron cloud covering at least two strips for a perpendicular incidence. Therefore, a minor deterioration resulted on the position resolution that was determined by a centre of gravity calculation.

The counters were mounted into gastight boxes having precision machined

orthogonal edges. Each box could contain two counters mounted orthogonally. For the beam test we used three boxes in which three detectors were mounted horizontally and parallel to each other (fig. 3). Two of the three counters had the same orientation, one was turned upside down. A fourth counter was mounted vertically to obtain the co-ordinate along the strips. The assembly of three boxes was sandwiched between two scintillation counters of 10x10 $cm^2$. The counters were aligned to the edges with an accuracy of 200 μrad. In section 3C the result of an alignment check with the beam is reported, which confirms this number. The s = 1.4 cm muon beam is well covered by the detectors.

The detector electrodes were set at the following potentials:

$V_{anode} = 0$ V, $V_{cathode\ strip} = -630$ V and $V_{drift\ electrode} = -2100$ V.

These values resulted into a drift field of about 6 kV/cm for the gas gap of 2.7 mm. At the present atmospheric pressure of 950 mbar a gas amplification of 1000 was measured and an average signal of 50,000 electrons for a perpendicularly entering particle. The connection of the strip pattern to the cathode voltage was designed such to minimise a possible damage from high voltage discharges. Therefore, the cathode strips were connected to the HV power supply in groups of 16 by a 4M7 resistor. The trip level was 70 nA. In this way, the cathode strips are isolated from the HV power supply for fast phenomena. Since the capacity between an anode strip and the adjacent cathode strips was only 6 pF the total discharge energy was limited to 19 μJ for a cathode strip voltage of - 630 V. However, as a drawback a signal from a single anode strip will induce a negative cross talk of 7% on the 15 neighbouring anode strips dedicated to the same group of cathode strips. By this phenomenon the tails of the ionisation cloud may be pushed down below threshold.

A second protection is provided by the MX5 inputs itself. Here an input resistor of 40 Ω is applied, followed by a diode/FET protection circuit to ground. The input resistor limits the peak value of the discharge current to 15 A, while most of the discharge energy is stored into the anode resistor instead of into the discharge itself and the preamp input.

Fig. 4 shows the architecture of the MX5 chip used as a preamplifier. The MX5 is designed to be used in the following way. The output of the integrating preamp is connected by a variable resistance R to two sample circuits which are controlled by the switches S1 and S2. Normally, both switches are closed. A short period before the event S1 is opened, preserving the baseline level in C1. After the event, when the voltage on C2 has adapted the new preamp level, S2 is opened as well. Hereafter, read out is accomplished by connecting the buffer amplifiers of C1 and C2 for each preamp channel sequentially to two output bus lines. A differential amplifier directs the subtracted signal to an FADC that is incorporated into a Camac Sirocco. Since for the MX5 the zero values of the individual channels are not equal, inside the Sirocco the pedestal is subtracted for each channel. Such a scheme is very useful for use at colliders like LEP where the moment of bunch crossing is very well known in advance.

However, for other experiments, like the one described here, no pretrigger signal is available and the event trigger arrives after a certain delay. The only way to cope with this situation, is to set R to a relatively large value, such that at arrival of the trigger the baseline level, which is stored into C1, is not significantly affected. However, this method inevitable leads to a certain loss of signal. For our set-up, we estimated the trigger delay at 120 ns. The rise time of the R/C2 circuit was set at 400

ns. For data acquisition a Macintosh II cx was used which could handle 100 events within the 2 s during beam burst. Using test pulses, the sensitivity of the data acquisition system was found to be 270 $e^-$ per ADC count.

From the pedestal fluctuations the rms of the output noise converted to the level of the MX5 input was measured to be 500 NEC at an anode load of 6 pF, resulting into a signal to noise ratio of 100. Since a part of the preamplifier chips had been mounted before on other prototype counters, several channels did not operate properly due to damage occurred during the interchanging.

## 3. Results

### a. Optimisation of the MX5 operation

For the operating scheme as described in section 2, the amount of signal loss was measured by comparison with events for which S1 was opened before the signal. This selection was realised by opening S1 with a fixed interval of 4 μs and recording only events within 3 μs after the last S1 opening. The signal amplitude measured in this operating mode appeared to be 25% higher than normal. Because the noise level was considerably higher we did not continue this randomly sampling mode. In another mode alternatively S1 and S2 were opened at a fixed rate to obtain a baseline sampling in either C1 or C2. This mode suffered likewise from an unacceptable high level of common mode noise.

### b. Homogeneity

The homogeneity of the detector is characterised by the variation of the gas amplification across the substrate. To determine this quantity, we did a measurement in the halo of the muon beam. From the recorded data for each MSGC the averaged amplitude was calculated over $2*10^5$ reconstructed tracks. For most channels the pedestal noise was about 2 ADC counts, a small number of them were over 5 counts. The charge from one track was distributed over more than one strip for many events. Therefore, only the summed amplitude from the cluster of all strips hit by the same track should be taken as the amplitude signal of the MSGC. To trace a cluster, initially a threshold of 30 ADC counts was applied onto the measured data. For the hit strips found in this way, the adjacent strips were traced using a threshold of only 15. Fig. 5 shows the measured cluster amplitude histogram of an MSGC using all channels. The familiar Landau distribution is apparent. The distribution has an average pulse height of 165 ADC counts (45 ke- ) and an rms width of 100.

Fig. 6 shows the measured averaged pulse height per strip across the substrate as a function of the strip number. Only averages containing at least 64 counts are displayed. Clearly the gas gain is at least almost constant for every channel. Due to an electronic error in the support board of the MSGCs, the last 60 - 80 channels could not be used. Therefore, only for an area of 350 channels the tracks could be detected by all three horizontal planes since one MSGC is turned upside down. A histogram of the averaged cluster amplitude across the full substrate is displayed in fig. 7. The rms of

the distribution is 5 %, a number that is reduced to 4 % by cutting five not properly working channels.

To determine the homogeneity of the gas gain along the strips, four regions of 17.5 mm long were defined. Using the data from the orthogonal counter, the amplitude measurements from the reconstructed tracks were classified into these regions. The result in fig. 8 shows that also in this direction the response is almost flat response with a minor decrease within the ± 1% region.

### c. Efficiency and position resolution

The cluster amplitude distribution displayed in fig. 5 shows that, even at a gas gain of 1000 and a rather high discrimination level of 30 ADC counts, only a minor fraction of the pulses is below threshold. This is quantified by determining the efficiency of a track through one of the central counters that has already been found by the three other MSGCs. For 97% of the tracks a hit within 300 μm from the predicted position was found. Correcting for the fraction of 1.6% broken preamplifiers, we obtain an actual efficiency of 98.4%.

Note that, in contrast to a broken preamplifier, an interrupted anode commonly does not lead to loss of efficiency. In such a case the isolated part of the anode will be charged up rapidly to a rather high negative voltage, directing the electrons to the neighbouring anodes. Therefore, in most events a broken anode will only result into a deterioration of the position resolution.

To determine the position resolution, tracks were fitted. At first, tracks were fitted through plane 2 and 4, using the well-defined direction of the particles in the beam halo. For these tracks, in plane 3 the position deviation was determined for the nearest hit deviating not more than 300 μm from the average deviation. Fig. 9 shows the deviation of the position measured in plane 3 from the position predicted by plane 2 and 4. The curve is not centred at zero since plane 2 was turned upside down and the counter position had not been aligned. From the distribution for the position resolution of a single MSGC an rms value of 52.5 μm is found, assuming that this parameter is equal for all three planes. This result is obtained from all fitted tracks. By cutting in the histogram 3% of the biggest deviations, caused by events supposed to originate from interrupted anode strips, the position resolution is improved to 45 μm. This number is still bigger than the value previously found [8] because the gas gap is smaller [9] and events affected by interrupted anodes were not skipped.

### d. Verification of the angular alignment

The events were classified into 4 regions along the strips in the way described in section 3A. For each region the residual of the position resolution was determined as the average over plane 2 and 4 diminished with the position found in plane 3. Accordingly the following values were found:

| strip region | residual (2;4)-3 (μm) | rms (μm) | # of events |
|---|---|---|---|
| A | 369 | 50 | 529 |
| B | 372 | 58 | 950 |
| C | 369 | 51 | 874 |
| D | 369 | 57 | 767 |
| Total | 370 | 55 | 3119 |

The table shows that the strips in plane 3 run parallel within a few μm to the strips in plane 2 and 4.

### e. High rate behaviour

Since the integration time of the preamps, as given by the time lag between the opening of the sample switches S1 and of S2, could not be adjusted below 700 ns without loss of signal, in the 20 MHz muon beam for each trigger an average of 15 clusters was observed. The histogram of the cluster amplitude (fig. 10) contains a multitude of very small values belonging to out of time particles. A considerable improvement of the spectrum occurs if only clusters are accepted from tracks that have been detected in all 3 parallel planes, like is shown in fig 11. Still the Landau curve of fig. 5 is not completely met, since out of time tracks have a certain chance to produce a hit in every plane as well.

The count rate histogram in fig. 12 displays nicely the profile of the muon beam while fig. 13 shows the distribution of the average cluster amplitude across the substrate. In the central region, the amplitude is slightly higher, which we attribute to pile up events of the 20 MHz beam within the 700 ns gate.
The measured position resolution amounts to 49 μm using the 3% cut, a number that is slightly worse than measured in the low intensity runs, possibly because of a contribution of a few out of time tracks.

### f. Spark damage

During the first days of operation, a few preamp channels died probably due to spark damage. The failure rate was of the order of 1%. Obviously, the protection resistor of 40 Ω at the preamp input does not in all events sufficiently limit the peak current of a possible discharge. After this period, in a cosmic set-up the detectors operated for a very long time without any further noticeable damage.

## 4. Conclusions

This test has shown, that the present MSGCs having an active area of 10 x 10 $cm^2$ and equipped with MX5 VLSI preamplifiers are operating satisfactorily for efficiency, position resolution and uniformity across the substrate. However, in future the MSGCs have to operate with the SMC trigger having a 700 ns delay instead of the 120 ns presently used. For the present MX5 chips this would result into many tens of ghost tracks due to the lack of a pipeline. Therefore, the MSGCs for SMC will be equipped with another type of preamp having a pipeline, the APC 64[10].

The applied HV protection gave a reasonable protection. The actual damage to the preamp channels is expected to diminish for a higher value of the input resistor to the preamp.

**Acknowledgements**

We thank L. Ceeli for the assistance during the test and likewise J. Severs, R van Dantzig and T.J. Ketel of the SMC collaboration for their co-operation during the runs.

## References


[1] A. Oed, Nucl. Instr. and Meth. A263 (1988) 351.

[2] R. Bouclier et al., High Flux Operation of Microstrip Gas Chambers on Glass and Plastic Supports, CERN-PPE/92-53, 20 March 1992.

[3] F. Angelini et al., A Microstrip Gas Chamber on a Silicon sibstrate, Preprint Univ. of Pisa, INFN PI/AE 91/10.

[4] M.H.J. Geijsberts et al., Tests of the performance of different gas mixtures in microstrip gas counters, Nucl. Instr. and Meth. A313(1992) 377.

[5] R. Bouclier et al., Development of Gas Microstrip Counters for radiation detection and tracking at high rates, CERN report DRDC 92-34, May 1992.

[6] P.P. Allport et al., A low power CMOS VLSI multiplexed amplifier for silicon strip detectors, Nucl. Instr. and Meth. A273 (1988) 630.

[7] Schott Desag D263 glass.

[8] M.H.J. Geijsberts et al., Optimization of the microstrip gas counter, Nucl. Instr. and Meth. A315 (1992) 529.

[9] J. Schmitz, Results on Monte Carlo simulations of a microstrip gas counter, Nucl. Instr. and Meth. A323 (1992) 638.

[10] R. Horisberger and D. Pitzl, A novel readout chip for silicon strip detectors with analog pipeline and digitally controlled analog signal processing, Nucl. Instr. and Meth. A326 (1992) 92.

## Figure captions

Fig. 1 Functioning of the MSGC.

Fig. 2 The assembly of the detector, complete with preamplifiers and control logic.

Fig. 3 Experimental set-up. The horizontal distances are exagerated to clarify the drawing.

Fig. 4 Architecture of the MX5 for one of the 128 channels.

Fig. 5 Measured cluster amplitude of all strips of an MSGC. The ADC threshold cuts the spectrum below 15 ADC counts.

Fig. 6 Measured average pulse height per strip as a function of the strip number.

Fig. 7 Distribution of the average cluster amplitude of all strips.

Fig. 8 Measured cluster amplitude (A) averaged over all strips as a function of the position (Y) along the strip. Y = 0 corresponds to the connection to the preamps.

Fig. 9 Deviation (X) in plane 3 between the calculated and the measured cluster position for beam tracks fitted through plane 2 and 4. The rms of the distribution corresponds to 52.5 μm per plane.

Fig. 10 Cluster amplitude of all strips of an MSGC measured in the 20 MHz muon beam.

Fig. 11 Cluster amplitude of all strips of an MSGC measured in the 20 MHz muon beam, but only for tracks detected in all 3 parallel planes.

Fig. 12 Histogram of the hit frequency in the muon beam.

Fig. 13 Average pulse height per strip as a function of the strip number measured in the 20 MHz muon beam.

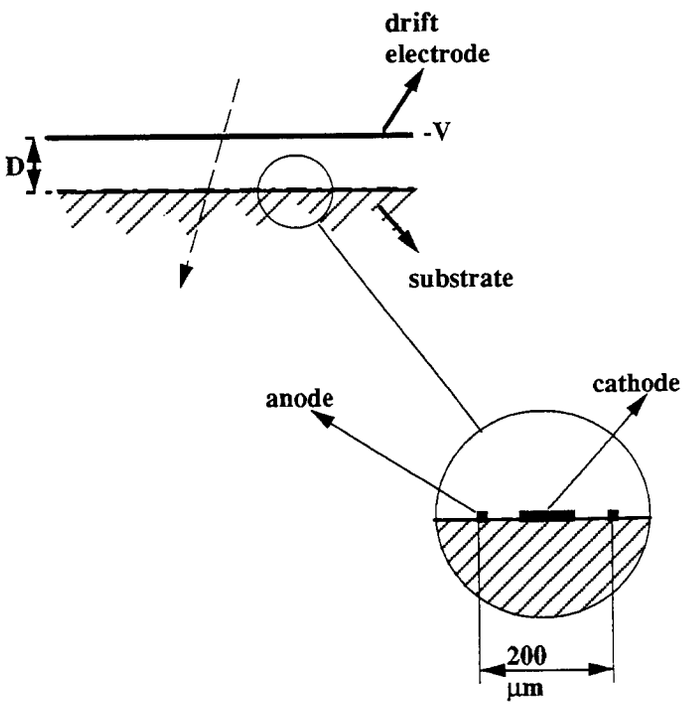


Fig. 1 Functioning of the MSGC.

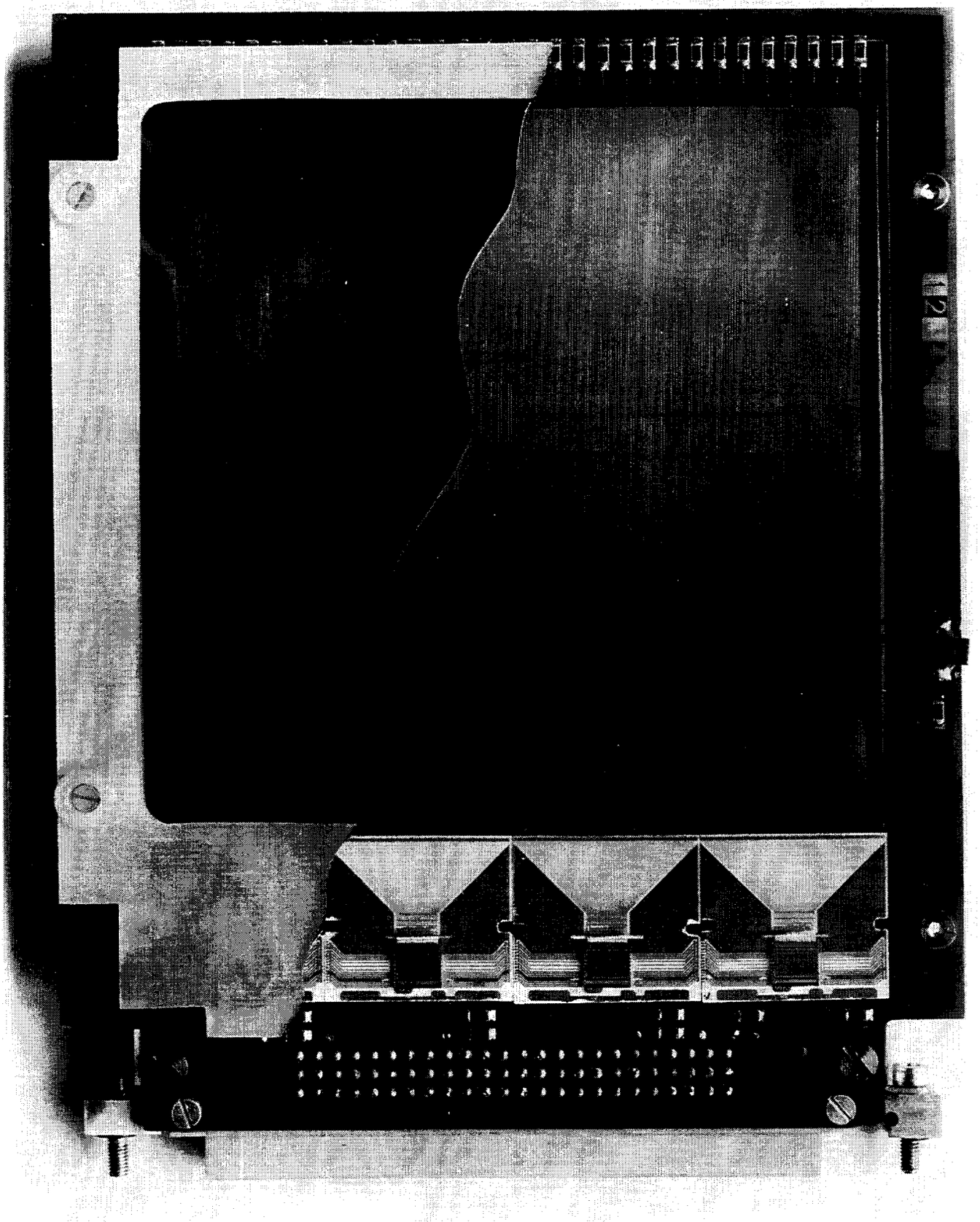

Fig. 2 The assembly of the detector, complete with preamplifiers and control logic.

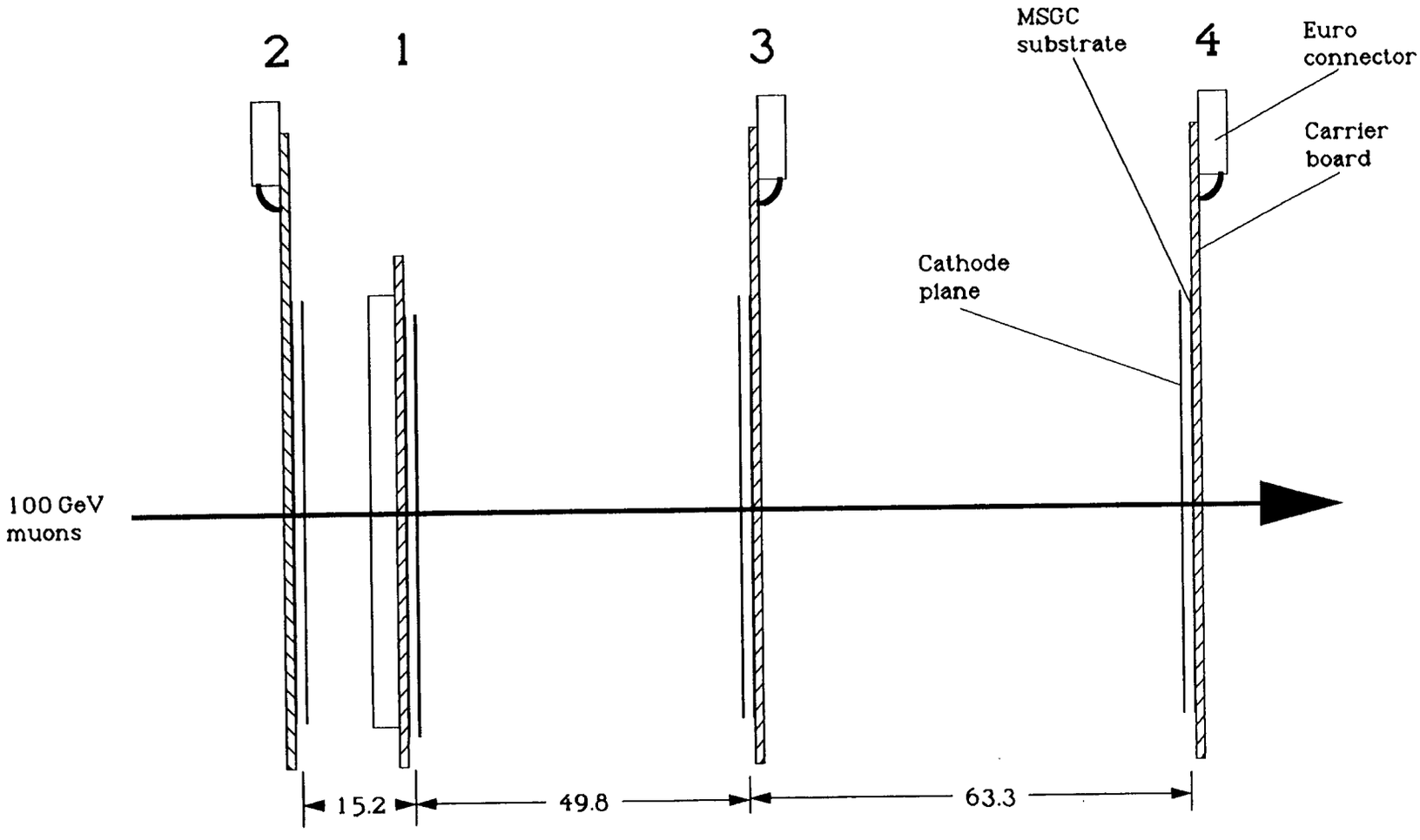


Fig. 3 Experimental set-up. The horizontal distances are exagerated to clarify the drawing.

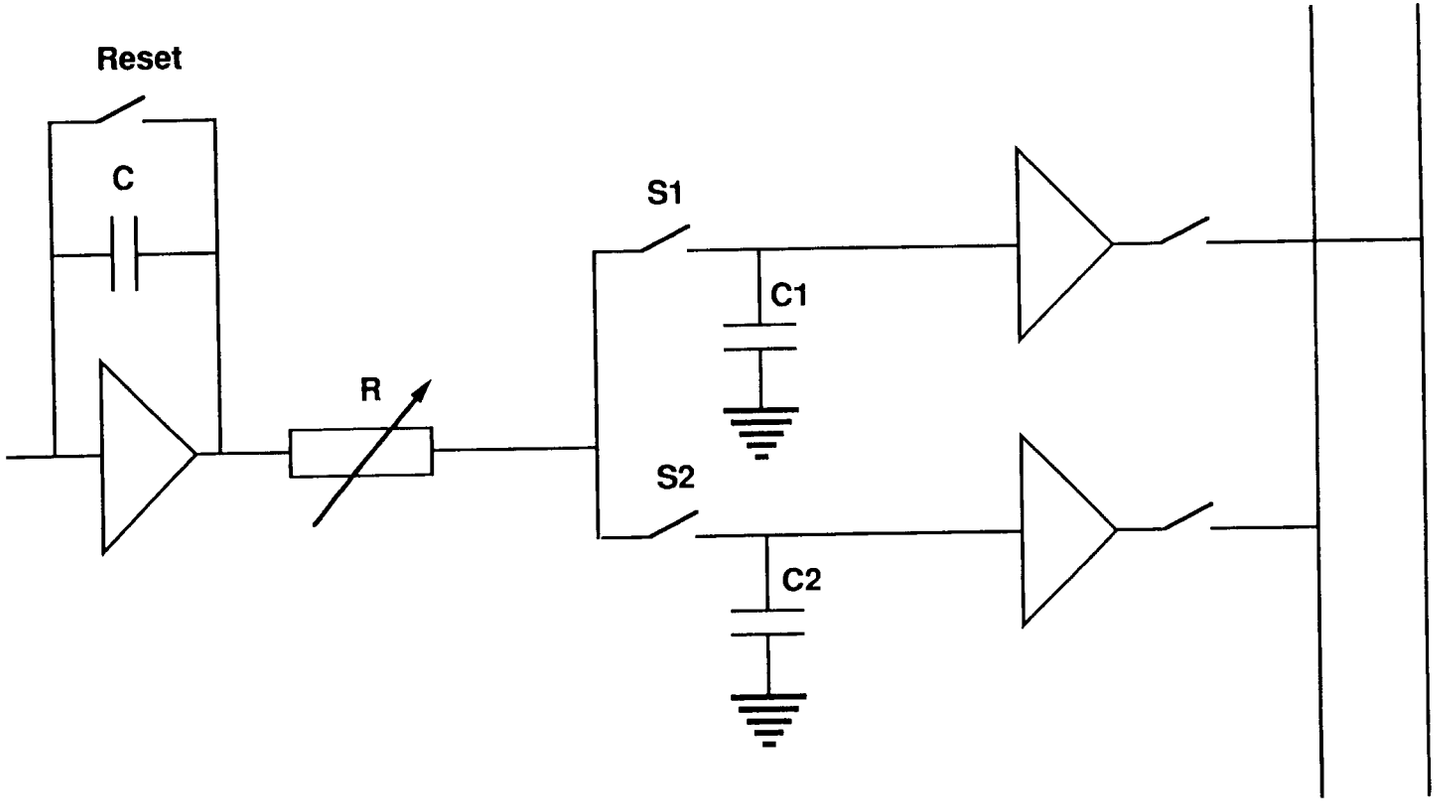


Fig. 4 Architecture of the MX5 for one of the 128 channels.

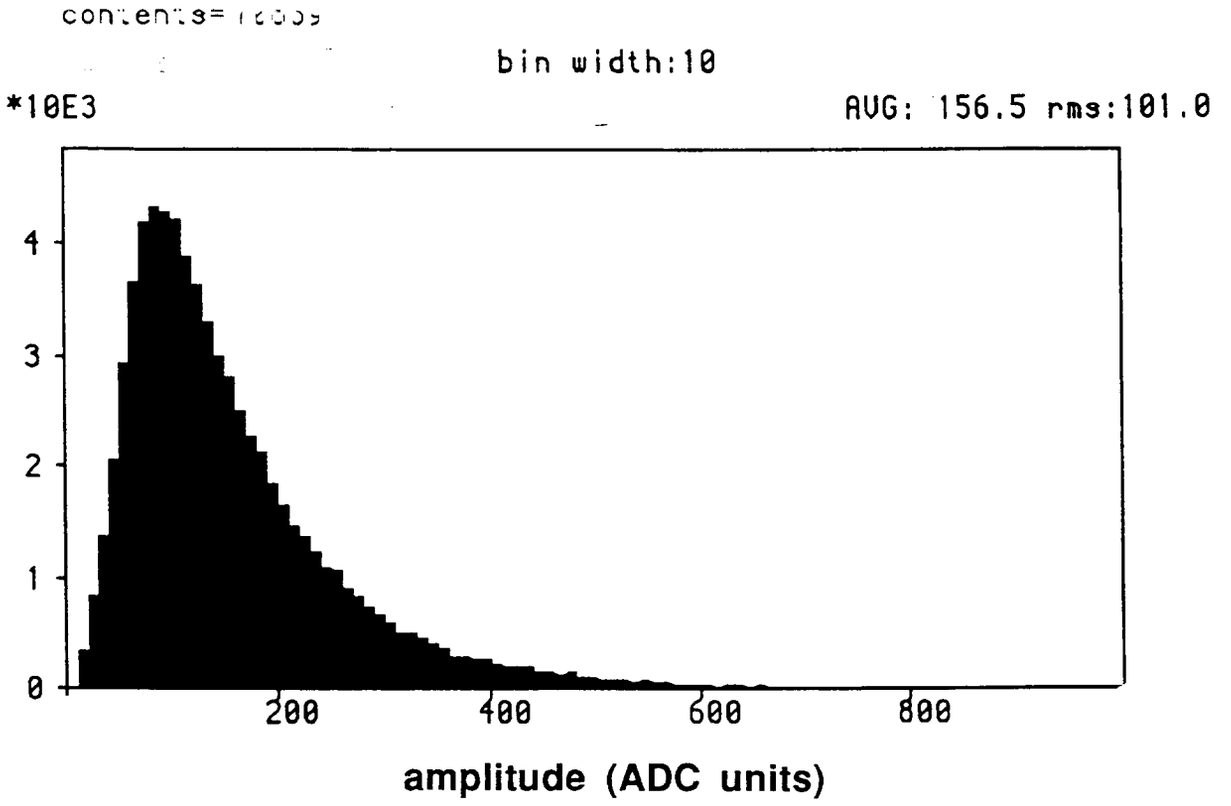


Fig. 5 Measured cluster amplitude of all strips of an MSGC. The ADC threshold cuts the spectrum below 15 ADC counts.

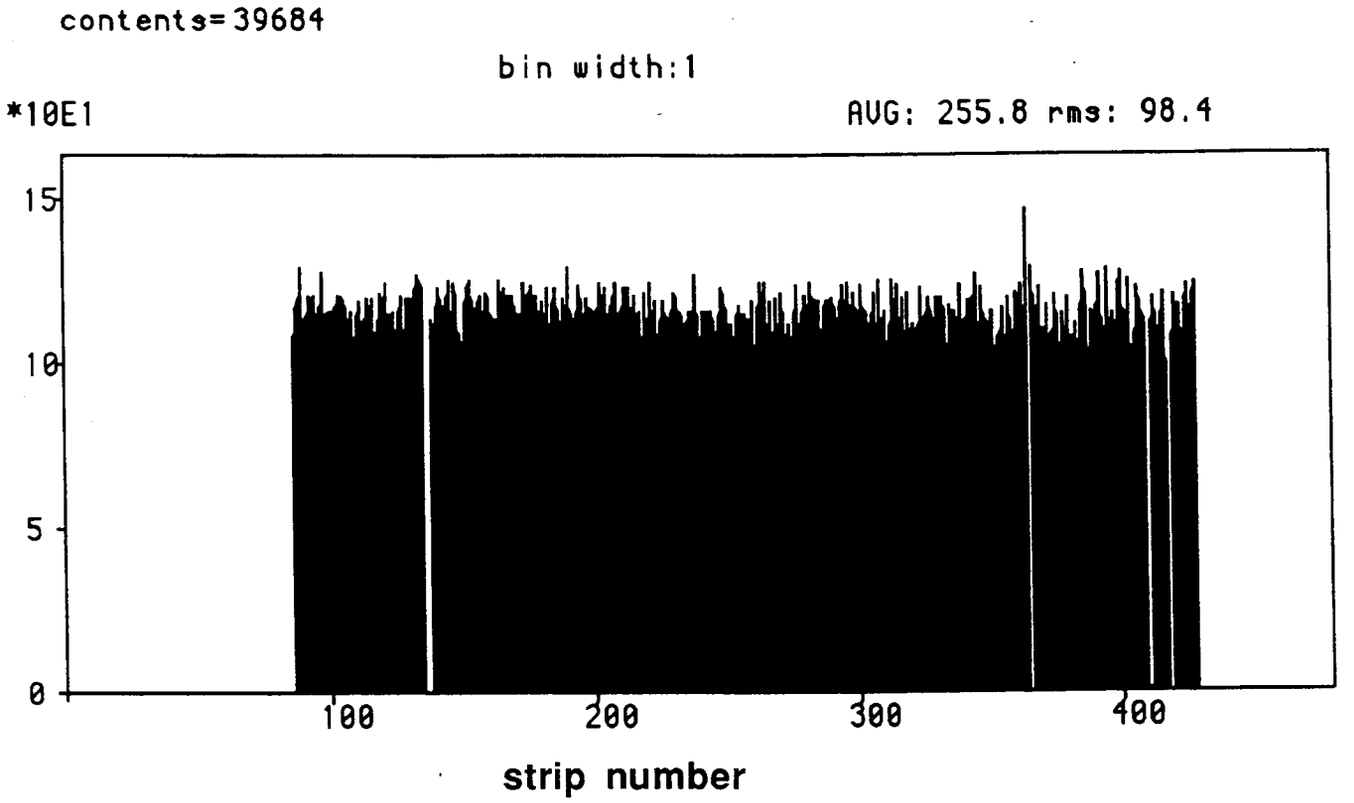


Fig. 6 Measured average pulse height per strip as a function of the strip number.

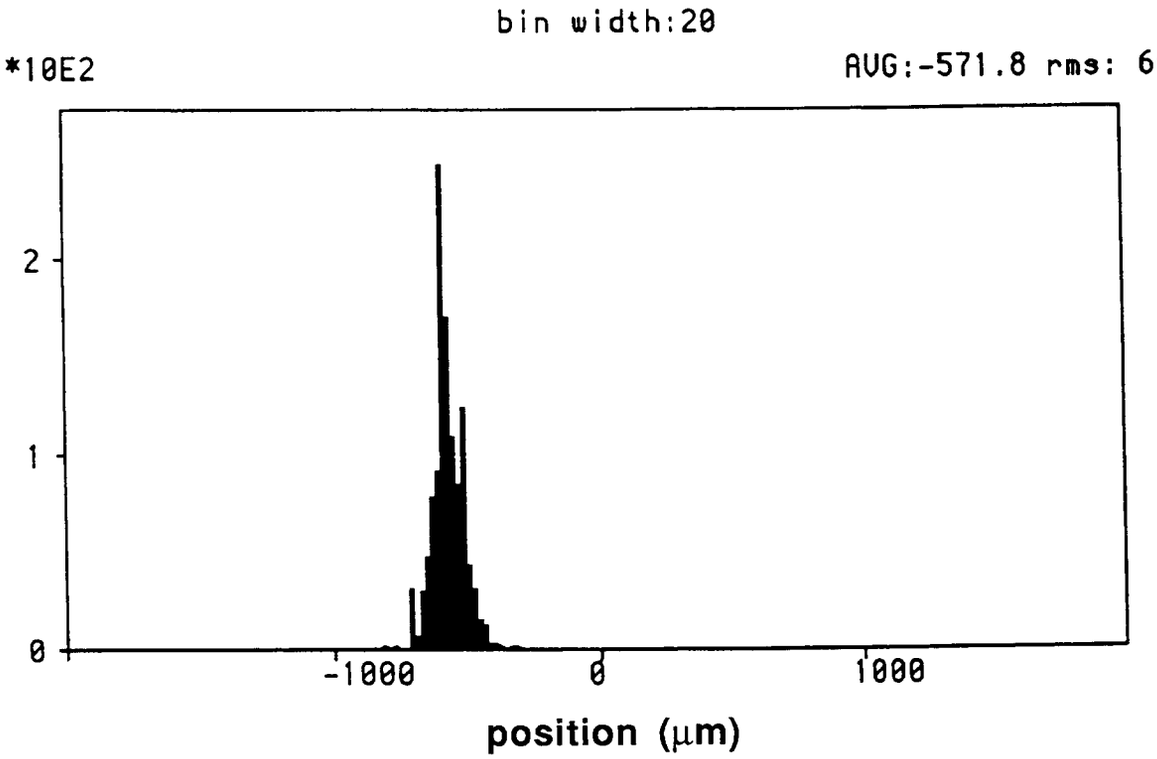


Fig. 7 Distribution of the average cluster amplitude of all strips.

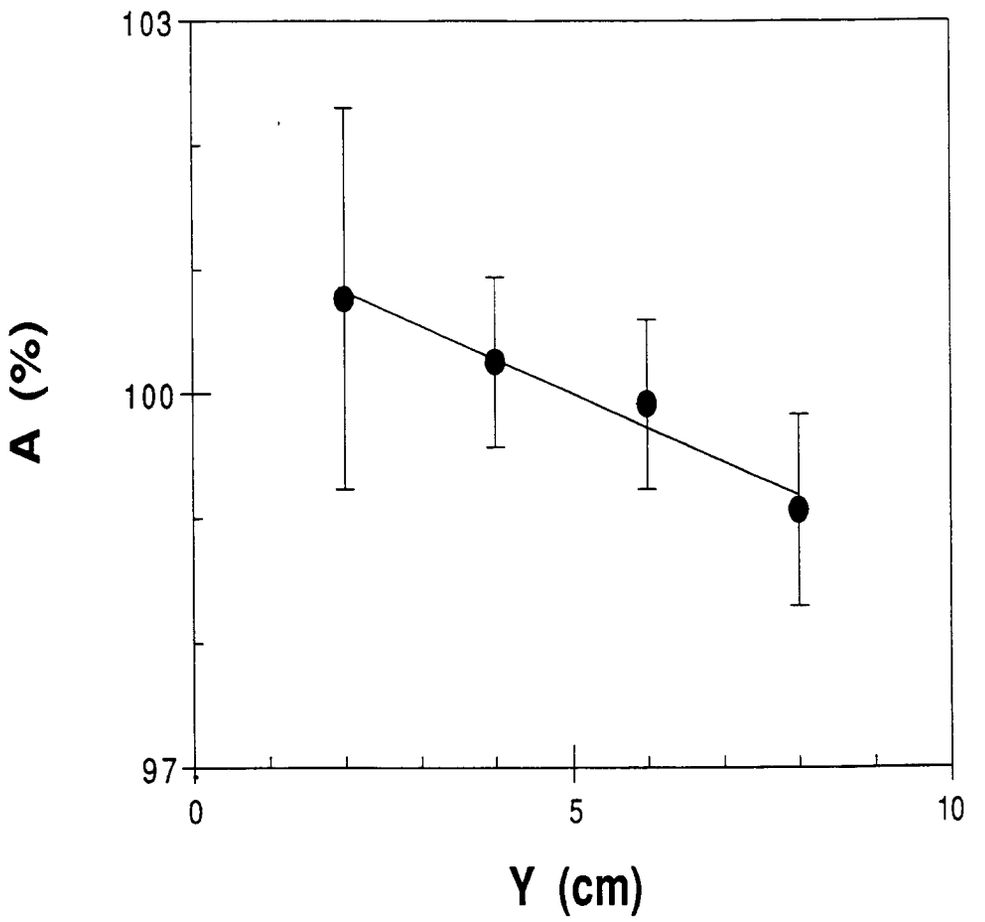


Fig. 8 Measured cluster amplitude (A) averaged over all strips as a function of the position (Y) along the strip. Y = 0 corresponds to the connection to the preamps.

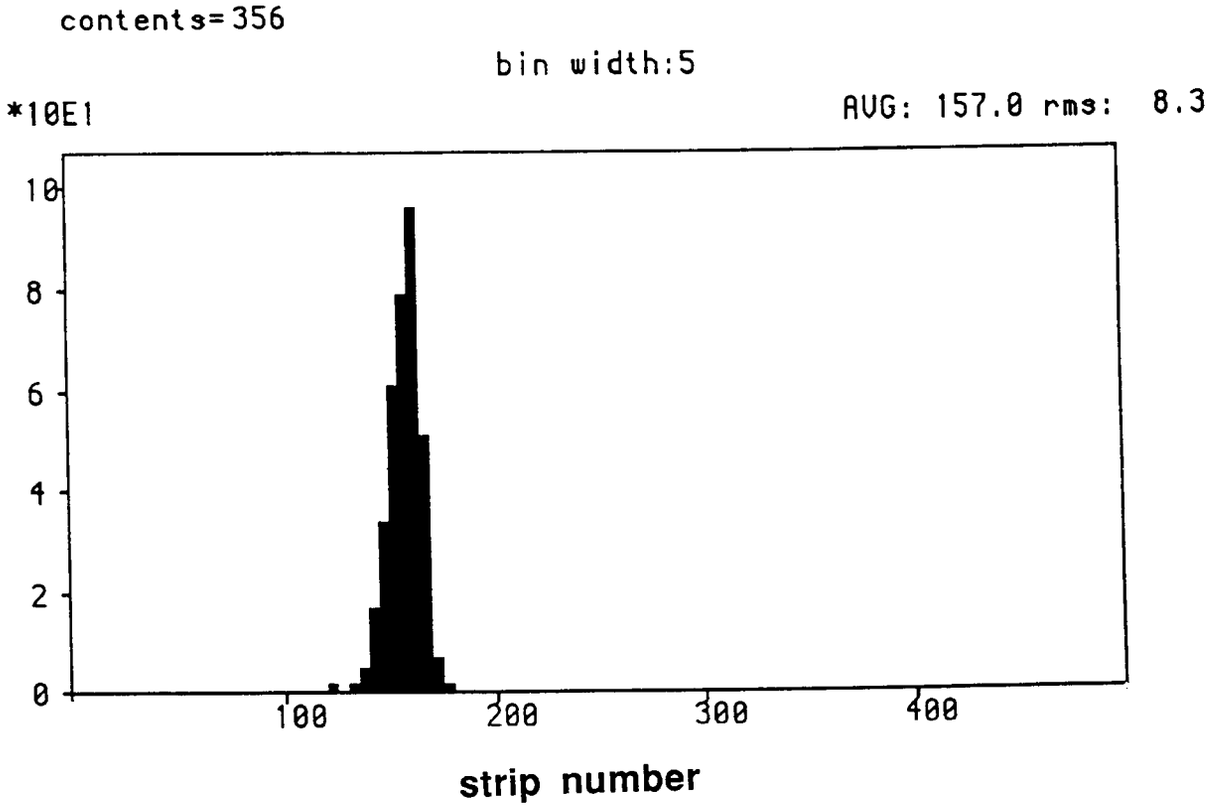


Fig. 9 Deviation (X) in plane 3 between the calculated and the measured cluster position for beam tracks fitted through plane 2 and 4. The rms of the distribution corresponds to 52.5 μm per plane.

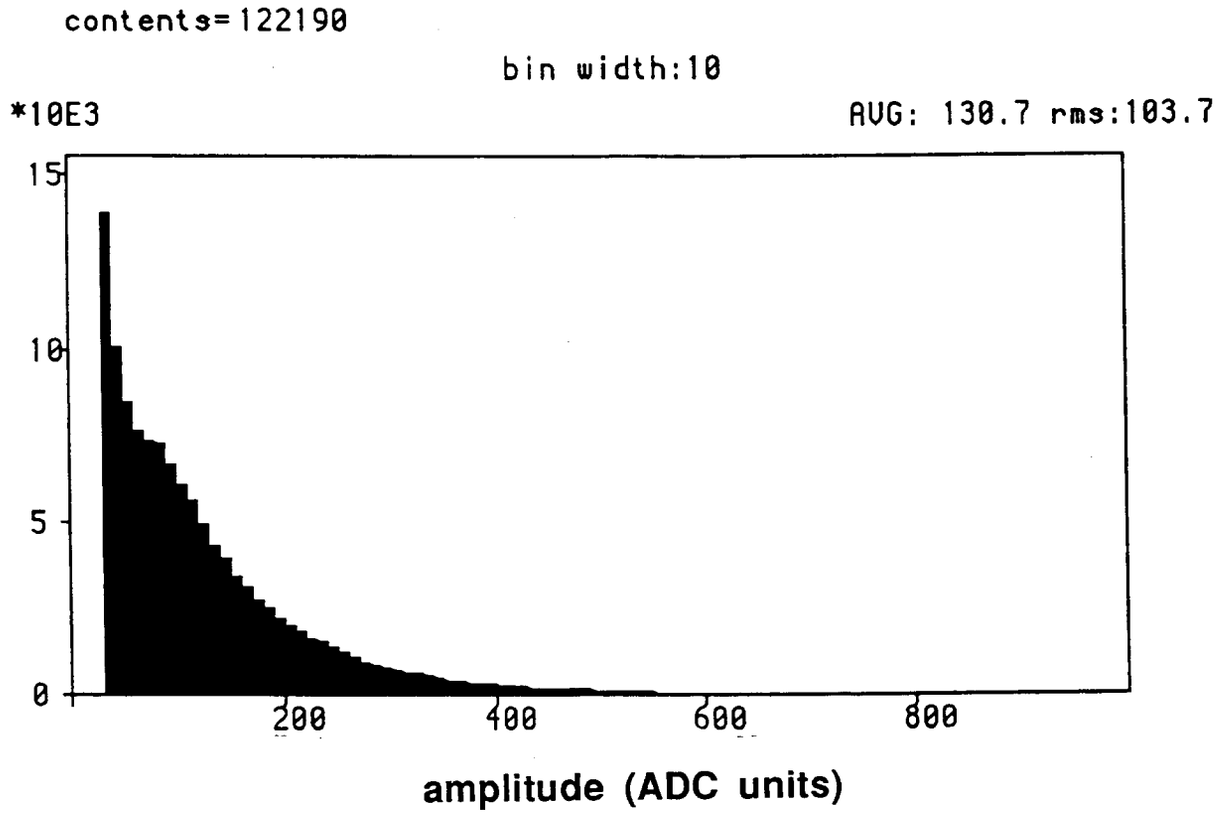


Fig. 10 Cluster amplitude of all strips of an MSGC measured in the 20 MHz muon beam.

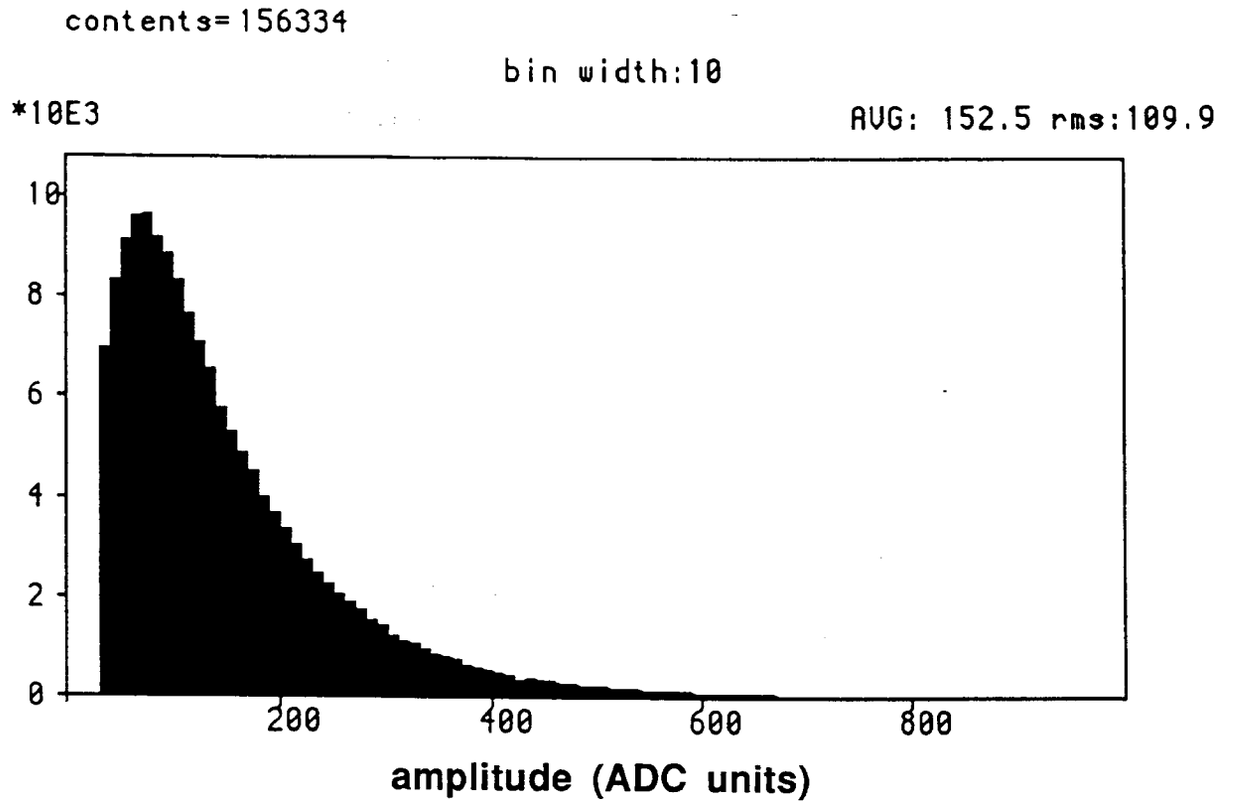


Fig. 11 Cluster amplitude of all strips of an MSGC measured in the 20 MHz muon beam, but only for tracks detected in all 3 parallel planes.

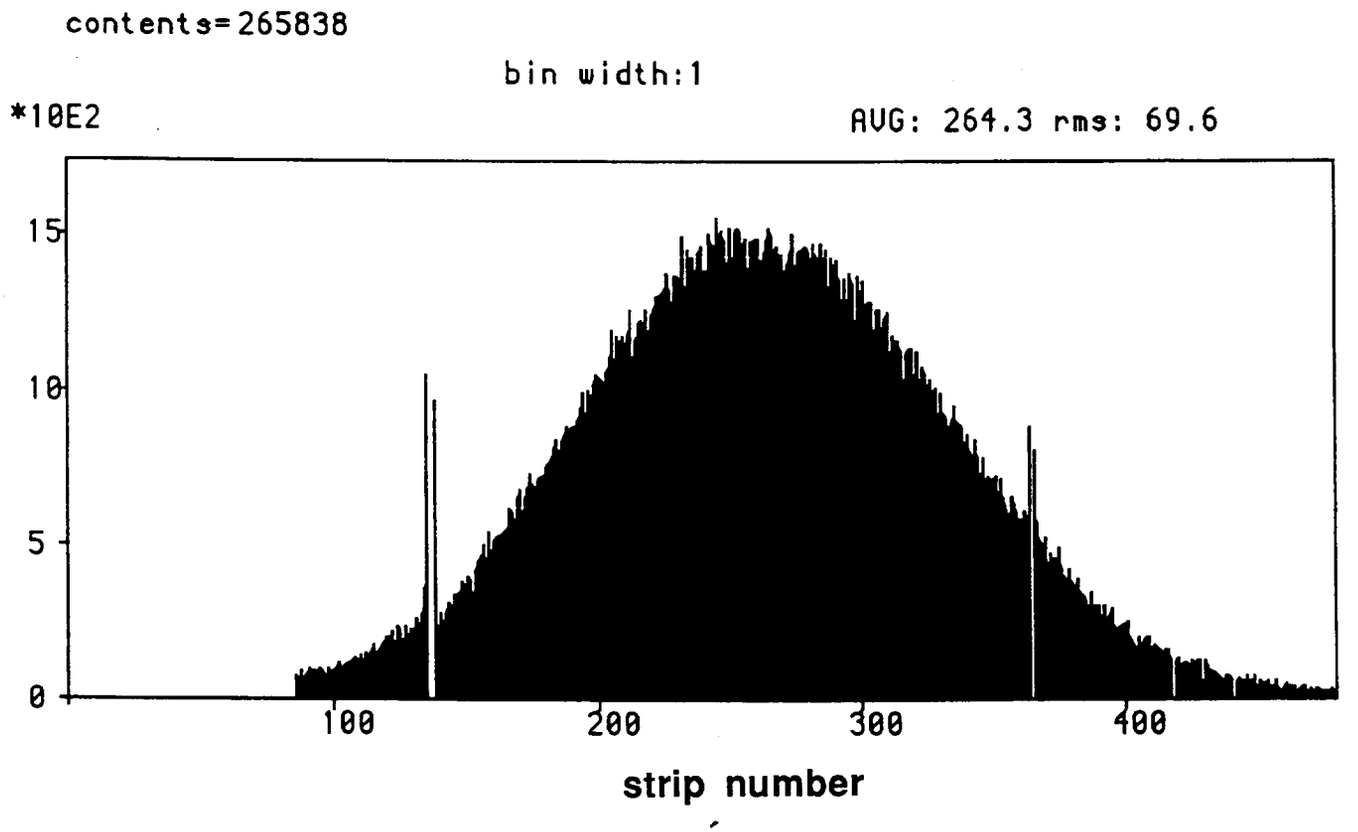


Fig. 12 Histogram of the hit frequency in the muon beam.

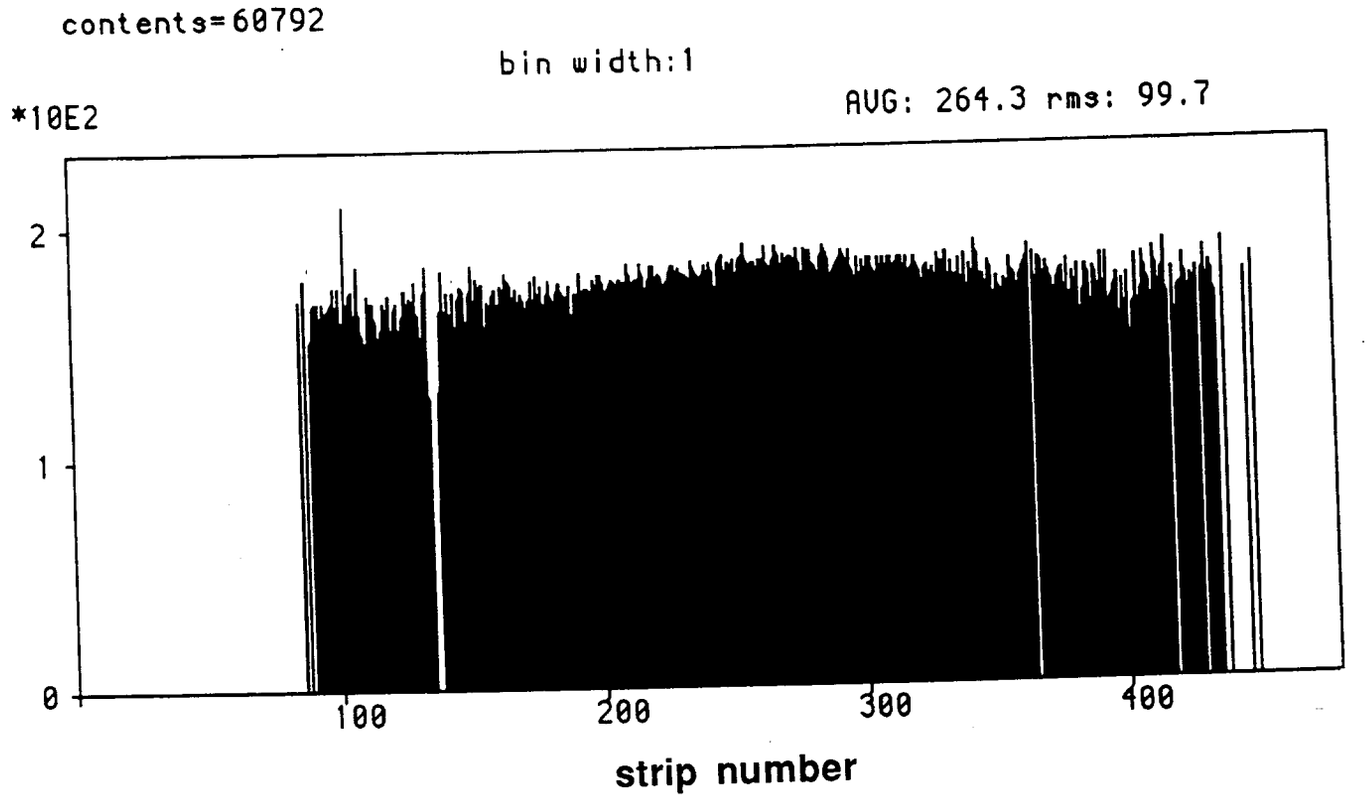


Fig. 13 Average pulse height per strip as a function of the strip number measured in the 20 MHz muon beam.